*March 1, 2013*
*Vladimir N. Litvinenko*
*Igor Pinayev*

# COHERENT ELECTRON COOLING EXPERIMENT AT IP2

*Abstract*

This white paper describes the present understanding of the extent and the scope of Coherent Electron Cooling Proof-of-Principle (CeC PoP) Experiment at IP2.

## I. Goal and Scope

The goal of the experiment is to demonstrate longitudinal (energy spread) cooling in CeC mode before expected CD-2 for eRHIC. Present scope of the experiment is to cool longitudinally a single bunch of 40 GeV/u Au ions in RHIC. The CeC experiment expected to be carried out during RHIC Runs 15 and 16 (and possible Run 17), with early commissioning of the accelerator during Run 14.

In addition to use for CeC demonstration experiment, the e-beam will be used for studying novel aspects of beam-beam effects in eRHIC by colliding the electron and hadron beams. These tests would be carried out after completion of CeC experiment.

## II. Location

The experiment will be located at IP2 (formerly the Brahms IP) and some equipment for the experiment will be located in a portion of Service Bldg. 1002A and 1002B.

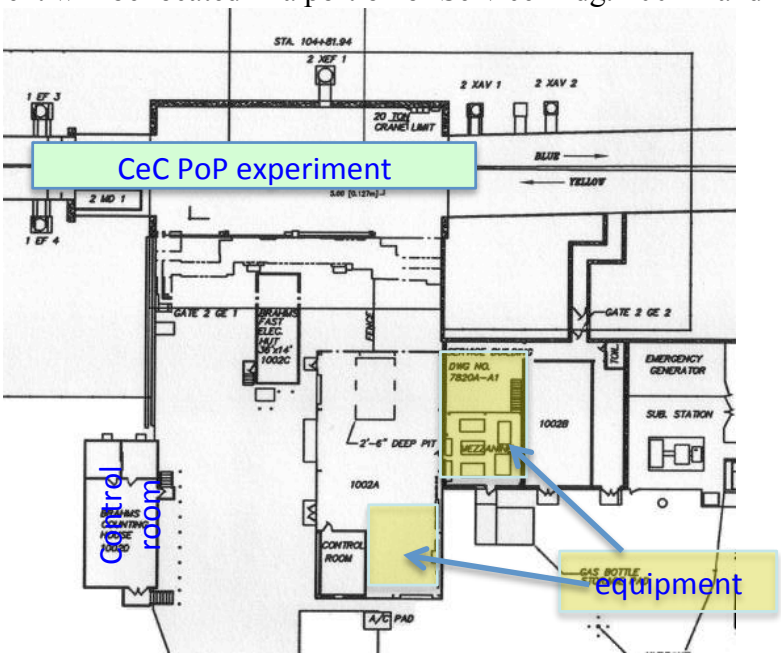


Fig. 1. Approximate location of CeC PoP experiment at IP2

Local control will be conducted, most likely, from a former Brahms Counting house, i.e. a trailer located at IP2.

## III. Schematic of the CeC

Fig. 2 is a schematic of a coherent electron cooler comprised of a modulator, a FEL-amplifier, and a kicker. The figure also depicts some aspects of coherent electron cooling. In CeC, the electron and hadron beams co-propagate in vacuum along a straight line in the modulator and the kicker and have the same velocity, v:

$$\gamma_o = E_e / m_e c^2 = E_h / m_h c^2 = 1/\sqrt{1 - v^2/c^2} >> 1 \qquad (1)$$

Since the electrons are about 2,000 fold lighter than a nucleon their energy is about the same factor less. For cooling Au ions with energy of 40 GeV/u we will use electron with energy of 21.8 MeV. Since the rigidity of the ion beam is in addition amplified by A/Z =197/79 ~ 2.5 fold, the effect of magnetic elements designed to transport electron beam has minuscule effect on the ion beam. In our case that magnetic elements (dipoles, trims and quadruples) affect the trajectory of electron beam 5,000 times stronger than that of the Au ion beam. This feature allows us to use common elements in the IP2 and to optimize lattice of the electron beam transport channel without affecting ion beam in RHIC.

The CeC works as follows: In the modulator, each positively charged hadron (with charge Z and atomic number A) induces a density modulation in electron beam that is amplified in the high-gain FEL; in the kicker, the hadrons interact with the electric field of the electron beam that they have originated, and receive energy kicks toward their central energy. The process reduces the hadrons' energy spread, i.e., cools the hadron beam.

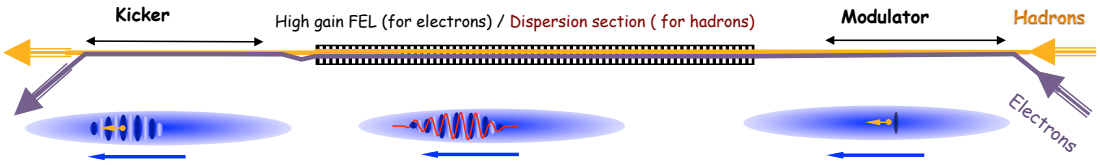


Fig. 2. Schematic of the CeC – economic option (see [1] for more details)

In practice, the scheme will look like that sketched in Fig.3 using most of the available space between two DX magnets at IP2. A 22 MeV linear accelerator will provide an electron beam, which will be merged with yellow Au ion beam circulating in RHIC. Both beams will co-propagate through the 14-meter (45-feet) long CeC system after which the electron beam will be separated from the yellow Au ion and damped.

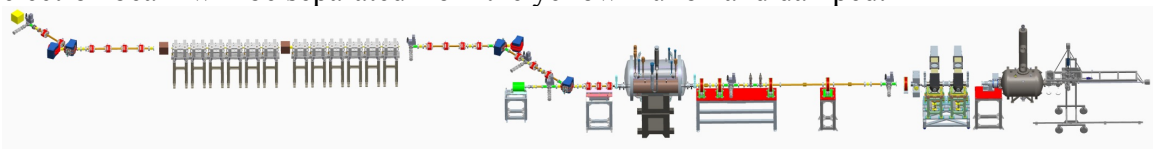

Fig. 3. Schematic of the CeC experiment at IP2.

Table 1 shows major electron and hadron beam parameters we plan to use for the experiment. Requirements for the quality of the electron beam and some FEL parameters are listed in the Table 2.

Table 1. **Main beam parameters for CeC experiment**

| **Parameter** | |
|---|---|
| Species in RHIC | $Au^{+79}$ ions, 40 GeV/u |
| Relativistic factor | 42.96 |
| Number of particles in bucket | $10^9$ |
| Electron energy | 21.95 MeV |
| Charge per e-bunch | 0.5-5 nC |
| Rep-rate | 78.17 kHz |
| Average e-beam current | 0.39 mA |
| Electron beam power | 8.6 kW |

Table 2. **Electron beam and FEL parameters**

| e-beam | |
|---|---|
| RMS Energy Spread | $\leq 1\times10^{-3}$ |
| Normalized Emittance | $\leq 5$ μm·rad |
| Peak Current | 60-100 A |
| FEL | |
| Wiggler Length | 7 m |
| Wiggler Period | 40±1 mm |
| Wiggler Strength, $a_w$ | 0.5 +0.05/-0.1 |
| FEL Wavelength | 13.6 μm |

## IV. Electron Accelerating Systems

Fig. 5 shows more details of a 22 MeV electron linear accelerator. The accelerator system comprises a 113.041 MHz superconducting RF (SRF) gun, operating on the 1446 harmonic of the RHIC revolution frequency, two 500.01 MHz 300 kV max copper cavities for ballistic bunching (h=6396), and 20 MeV 704.04 MHz superconducting RF cavity (h=9006).

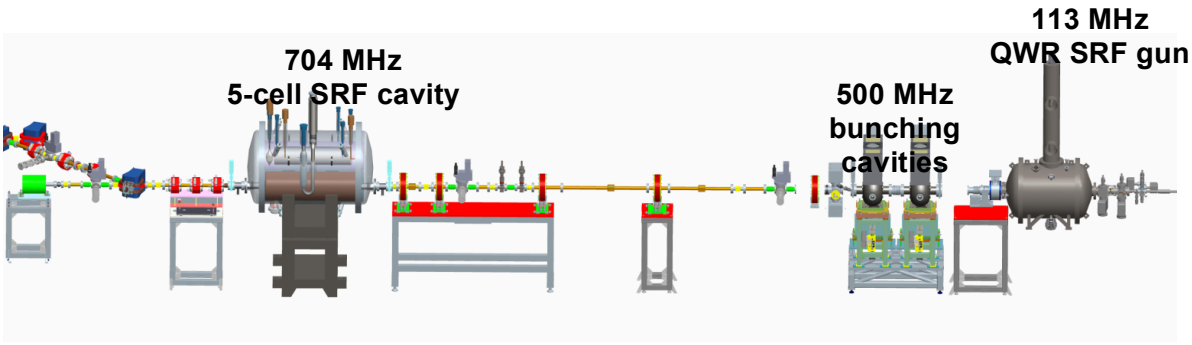


Fig. 4. 3D rendering of the 22 MeV accelerator.

The 100-300 picoseconds long, 2 MeV electron beam generated the SRF gun goes through the bunching cavities, where electron acquire energy chirp. Alternatively the electrons can be generated off-crest to utilize distance between gun and bunching cavities for compression.

After bunching to about 10-20 psec in the drift section, electrons are accelerated to 21.95 MeV (total energy) in 5-cell SRF cavity and pass through an achromatic dogleg to join the "yellow" Au beam. After passing through the CeC section, electron beam is separated from the ion beam by a dipole, which directs it into the beam dump.

## SRF Gun

Electrons are generated at the CsKSb photo-cathode, which is inserted into the 112 MHz quarter-wave SRF cavity from the back of the cryomodule (see Fig. 5). It allows to generate long electron bunches to reduce space charge effect. The design provides short accelerating gap with almost constant accelerating field.

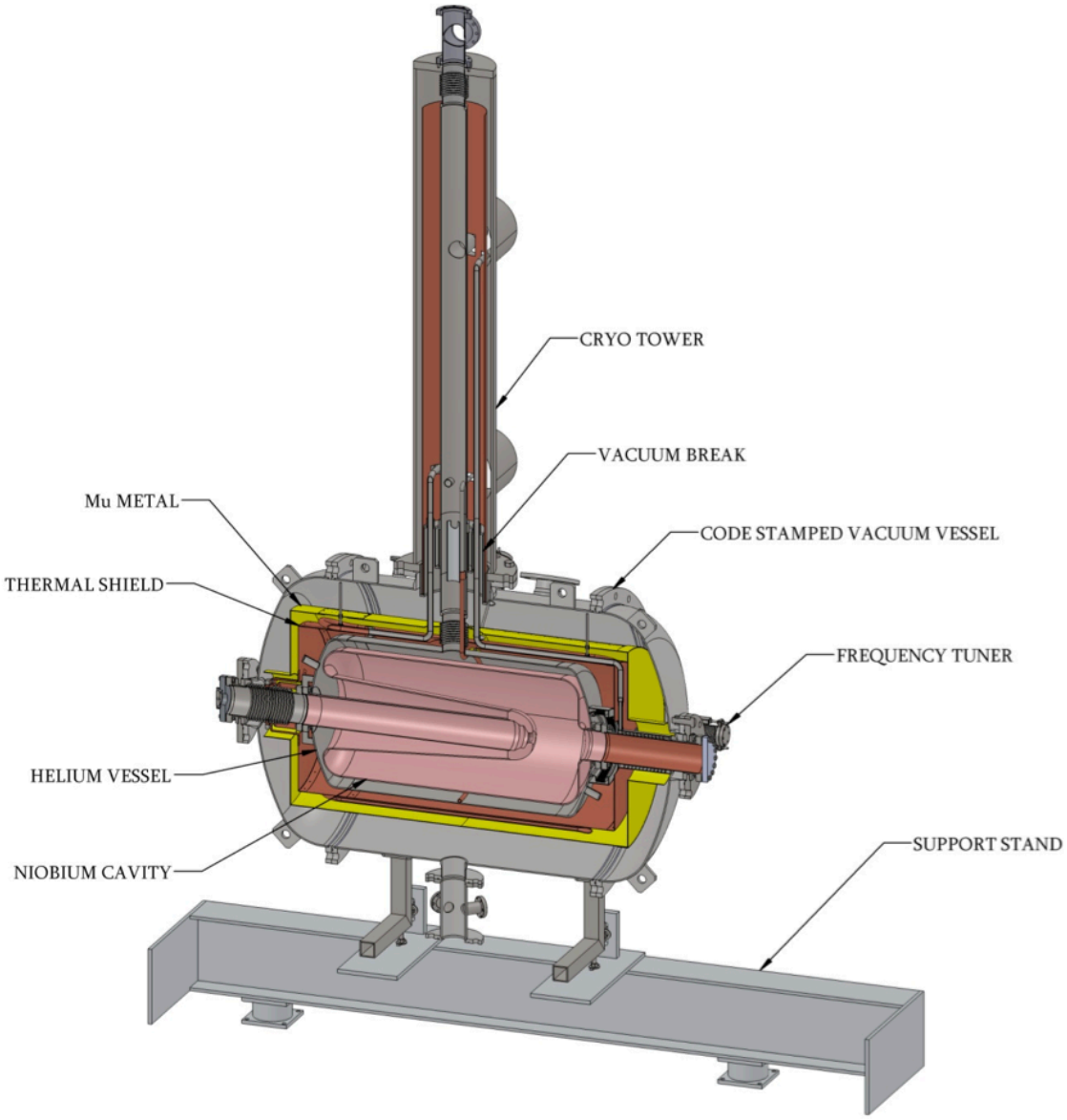


Fig. 5. The 113 MHz photo-injector with cathode stalk insertable from the back of the cryomodule. The cathode is illuminated by a green light from a laser (not shown in the figure). The cavity has a quarter-wave structure, with coaxial fundamental power coupler, which also serves as a fine tuner. Here electrons travel from left to right.

The laser will deliver 100 ps to 500 ps long pulses of green light to the surface of the photocathode and generate near-flat top e-beam profile.

The 113 MHz SRF gun has undergone modifications by Niowave Co. (see Fig. 6), while the cathode stalk and transport system is under production by Transfer Engineering. The fundamental power coupler (FPC) for this cavity is designed and will be manufactured.

Fig. 6. Picture of the SRF gun after repackaging at Niowave before installation of the chimney.

The SRF gun parameters are shown in Table 3.

Table 3. SRF gun parameters

| Parameter | Value |
|---|---|
| Beam aperture | 10 cm |
| Operating temperature | 4.5 K |
| Nominal accelerating voltage | 2.0 MV |
| Peak electric field | 38.2 MV/m |
| Field at the cathode | 14.5 MV/m |
| R/Q | 127 Ohm |
| $Q_0$ | $4.6 \times 10^9$ (measured at low gradient) |
| RF power loss | 12.3 W |
| $Q_{ext}$ | $10^7$ |
| Tunability by frequency tuner | ±40 kHz |
| Peak detuning due to microphonics | 6 Hz |
| Available RF power | 2 kW |
| Beam power | 780 W |
| Tunability with power coupler | ±2 kHz |

Niowave on December 17-19, 2012 provide tests of the modified cavity. Quick cooling was reached to avoid Q disease. The static heat load was measured 6 W. The nominal fundamental frequency is 113.05 MHz, with expected operational value of 113.04 MHz

(h=1446). The fundamental frequency will be adjusted using coarse tuner (see Fig. 7). The dependence of fundamental frequency on the atmospheric pressure was found 8.1 Hz/mbar.

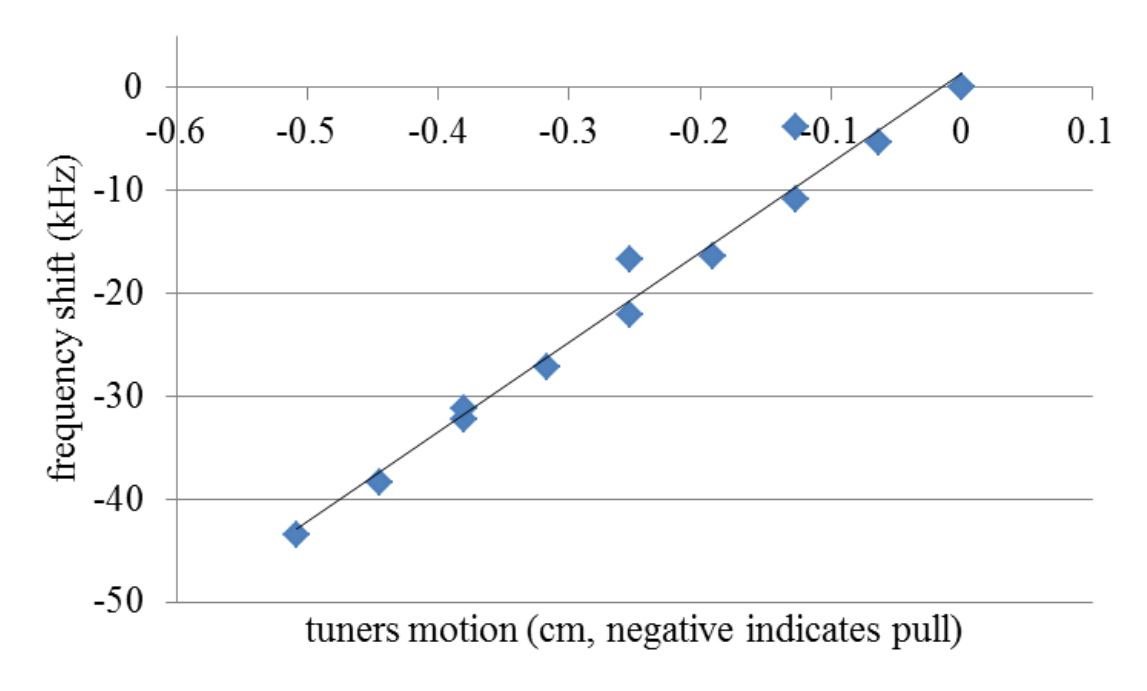


Fig. 7. Test of coarse tuner operation. The slope of the line is 87.1 kHz/cm.

The power for the SRF gun will be provided via a fundamental power coupler (FPC), which will also serve as a fine tuner, providing about 4 kHz tuning range with ±2 cm travel range. The tip of the FPC in the extreme position (about 1 cm from the cavity gap) will have more than 1 kW power dissipated and will be water-cooled.

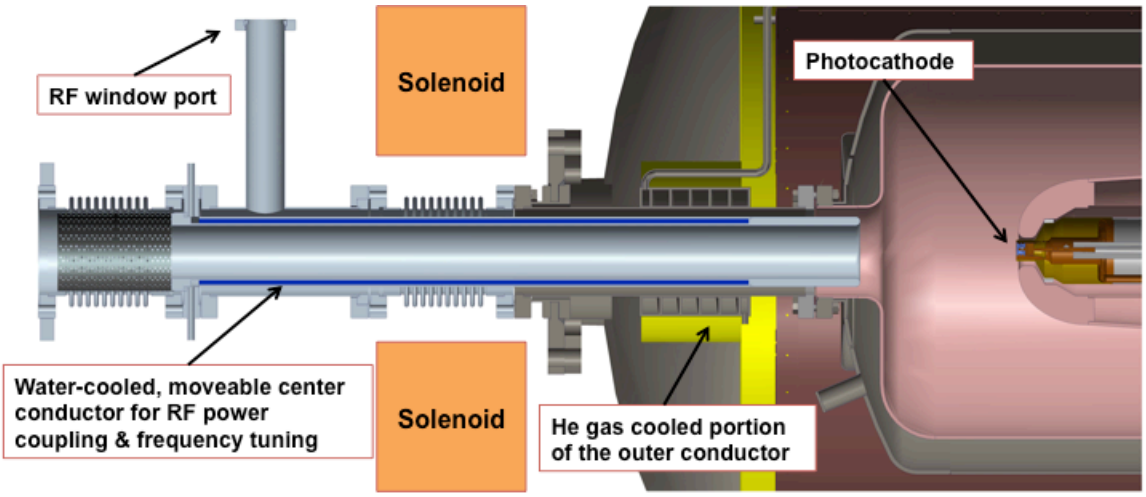


Fig. 8. Design of the fundamental power coupler.

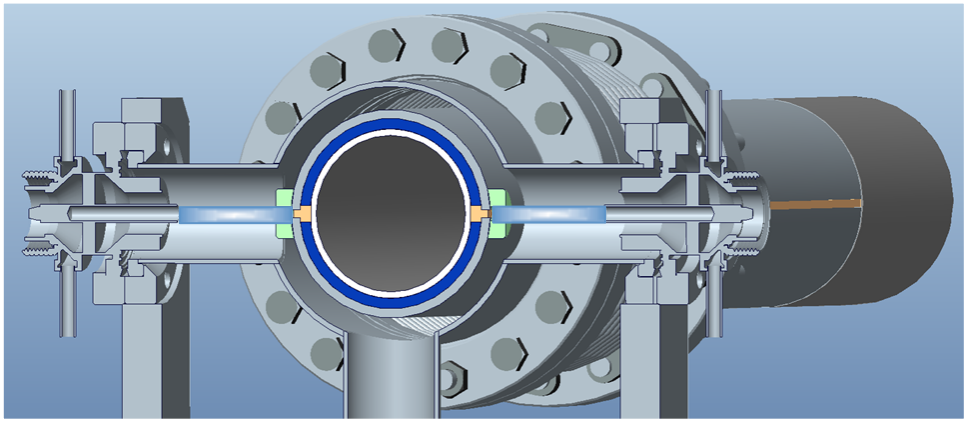

Fig. 9. View of the vacuum feed-through for connection of the coaxial cable to the FPC. The lower pipe will be used for connection of the ion pump.

Transmitter for the gun is built by Tomco Technology, which realized as class AB 2 kW linear amplifier. The circulator is made by Ferrite Microwave and has port 3 terminated. Both transmitter and circulator are installed into the standard 19" rack (see Fig. 10).

Fig. 10. 19" rack with mounted 2 kW amplifier and circulator.

## 500 MHz Cavities

Two 500 MHz room temperature cavities (see Fig. 11) will give energy chirp to the electron beam. Each cavity can provide up to 300 kV RF voltage to provide the necessary chirp. The chirp creates the velocity difference, with the electrons at the head of the bunch having lower velocities that that at the tail.

The cavities will be fed by a transmitter (under purchase from Thomson Broadcast Co) via an AFT microwave's circulator and a power splitter.

Both 500 MHz cavities require room temperature water-cooling.

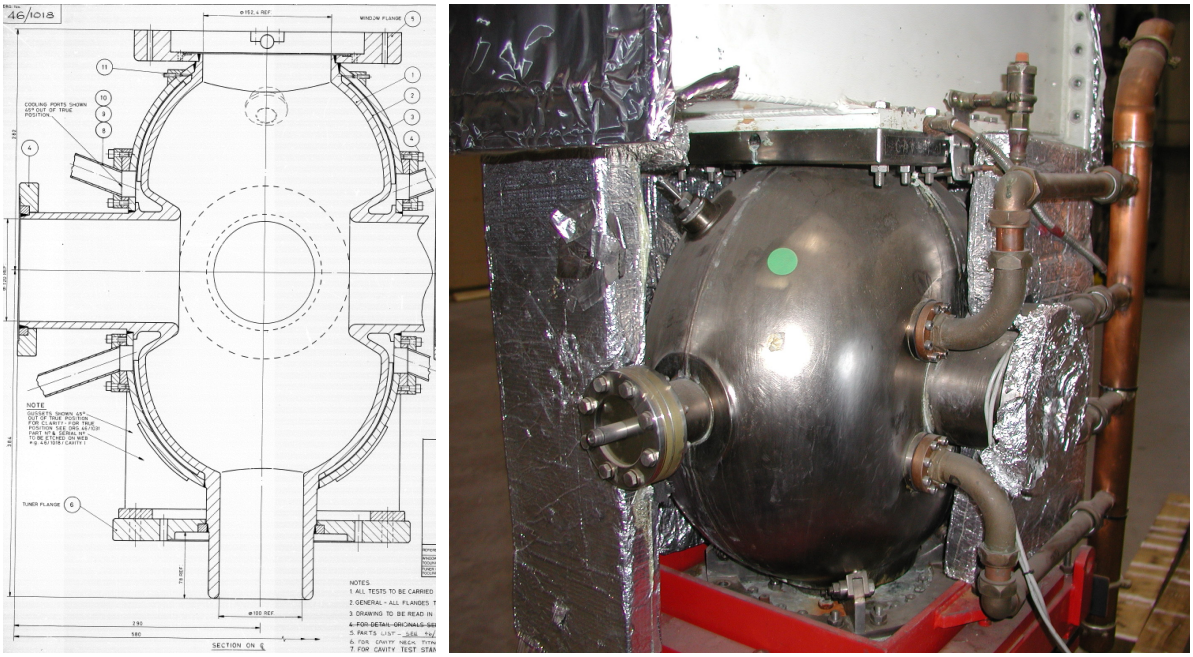

Fig. 11. Design and view of the 500 MHz copper RF cavities from Daresbury Lab.

Table 4. Parameters of the 500 MHz cavities

| Parameter | Value |
|---|---|
| Accelerating voltage | 300 kV |
| R/Q | 178.5 OHm |
| Geometry factor | 38.2 Ohm |
| $Q_0$ | 31,000 |
| RF power losses at maximal voltage | 16.3 kW |
| Available RF power | 50 kW per cavity |
| Tuning range | kHz |

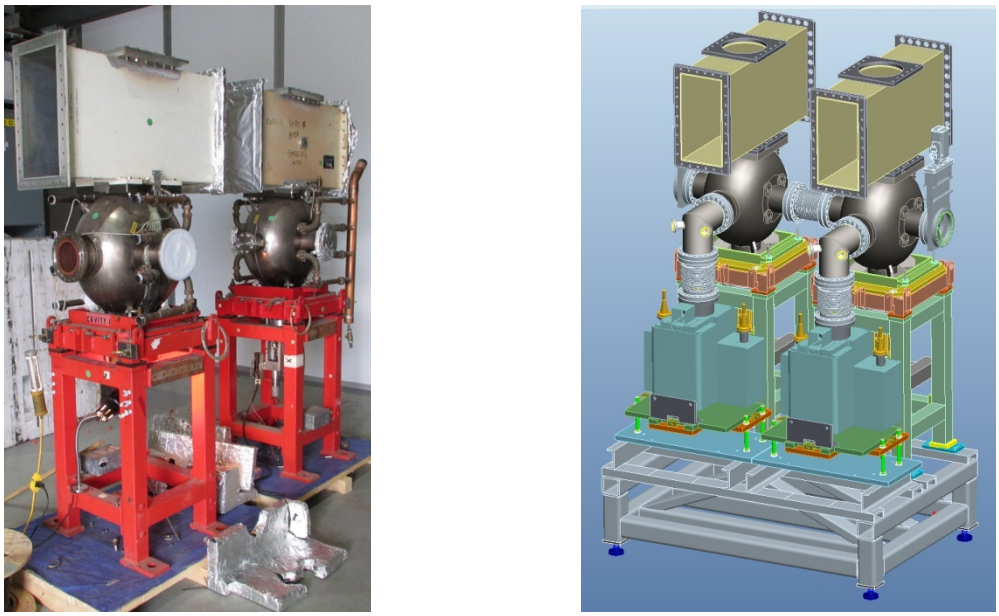

Fig. 12. View of the cavities on supports and proposed installation for the CeC PoP experiment.

The bunching cavities will be fed from a 50 kW transmitter built by Thomson. Fig. 13 shows view on the transmitter and IOT in the bay area.


Fig. 13. View of the 50 kW transmitter for 500 MHz system.

## 704 MHz System

A 5-cell SRF linac, named BNL3, working at 704 MHz will serve as the main 20 MeV accelerator. The BNL3 704 MHz SRF linac cryostat is in a design stage, the niobium 5-cell SRF structure was manufactured at AES. Niowave will build similar structure and after tests the best cavity will installed into the cryostat by Niowave.

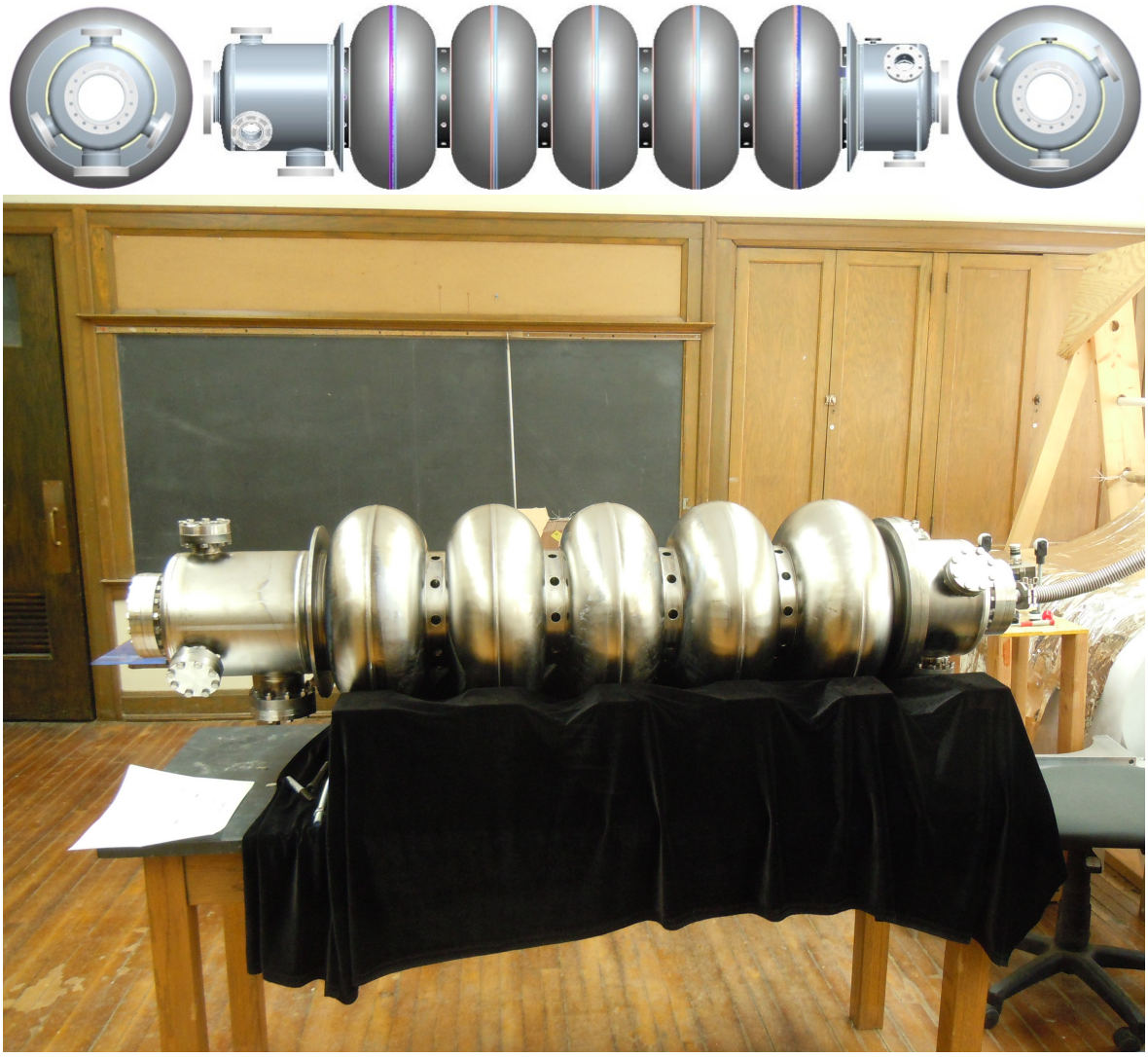

Fig. 14. Top: Design of 5-cell 704 MHz BNL3 SRF linac (without the cryostat). Bottom: BNL3 5-cell cavity at Niowave.

The 704 MHz system is supposed to be fed from 20 kW amplifier from Bruker (see Fig. 15).

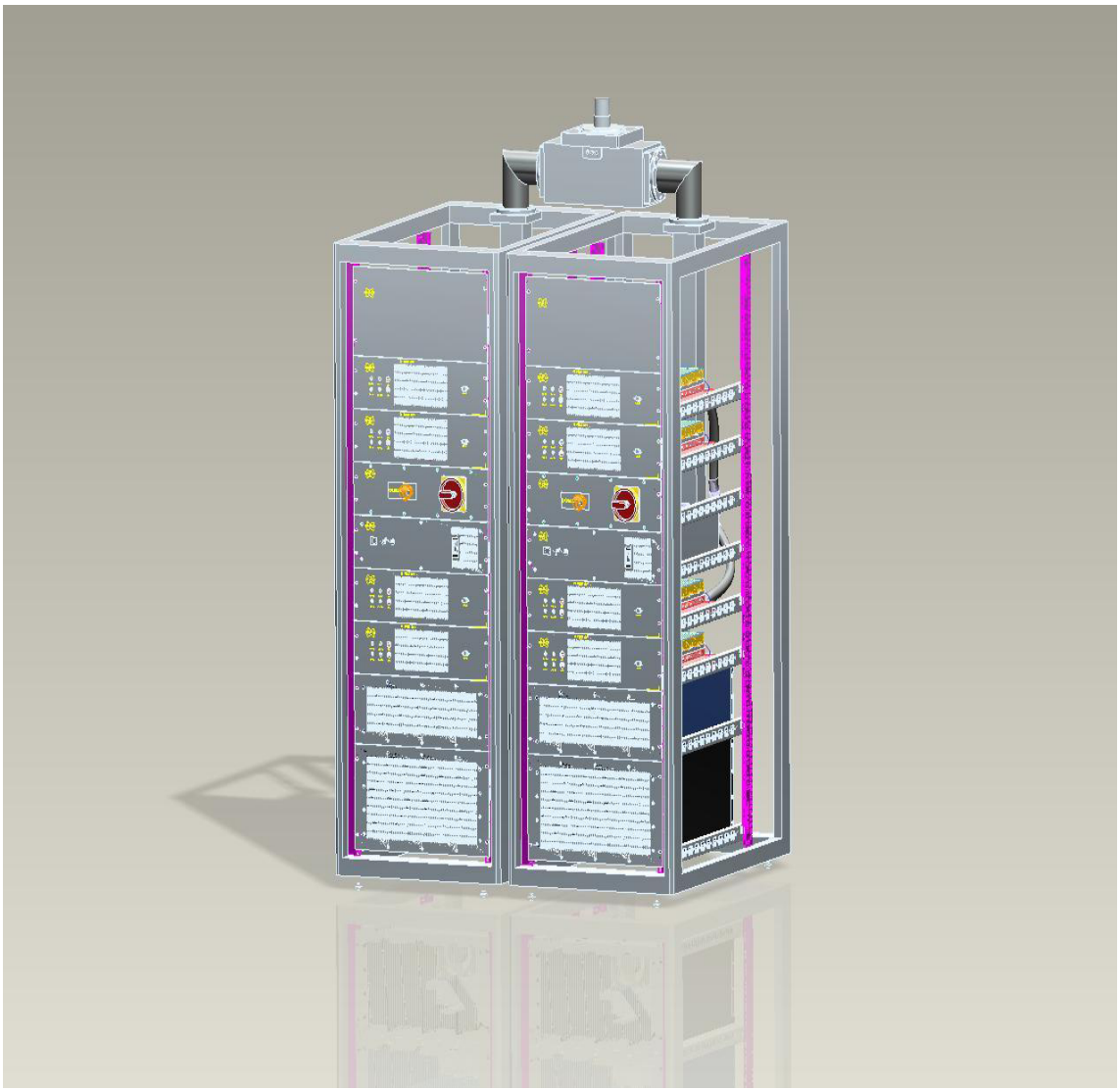

Fig. 15. 3D rendering of the 20 kW transmitter for 704 MHz system.

The low-level RF system for CeC PoP is based on the LLRF Upgrade Platform already successfully deployed at RHIC, AGS, EBIS and the ERL experiment. All necessary clock and frequencies (78 kHz revolution clock, 113 MHz, 500 MHz, 704 MHz) will be generated locally from the 100 MHz reference frequency brought from IP4.

## V. Cryogenic System

The coherent electron cooling experiment will utilize two cryogenic systems. The SRF gun with the 113 MHz fundamental frequency will use 4.4 K cryogenic system, which will contain a phase separator and a quiet helium vessel (see Fig. 16). The 704 MHz accelerator cavity will employ 2K cryogenic system with a superfluid heat exchanger and a phase separator. Liquid helium will be supplied to the CeC PoP system from a local tap off the RHIC cryogenic distribution system. Any pressure oscillations from the RHIC distribution system will be buffered by the phase separator's vapor volume.

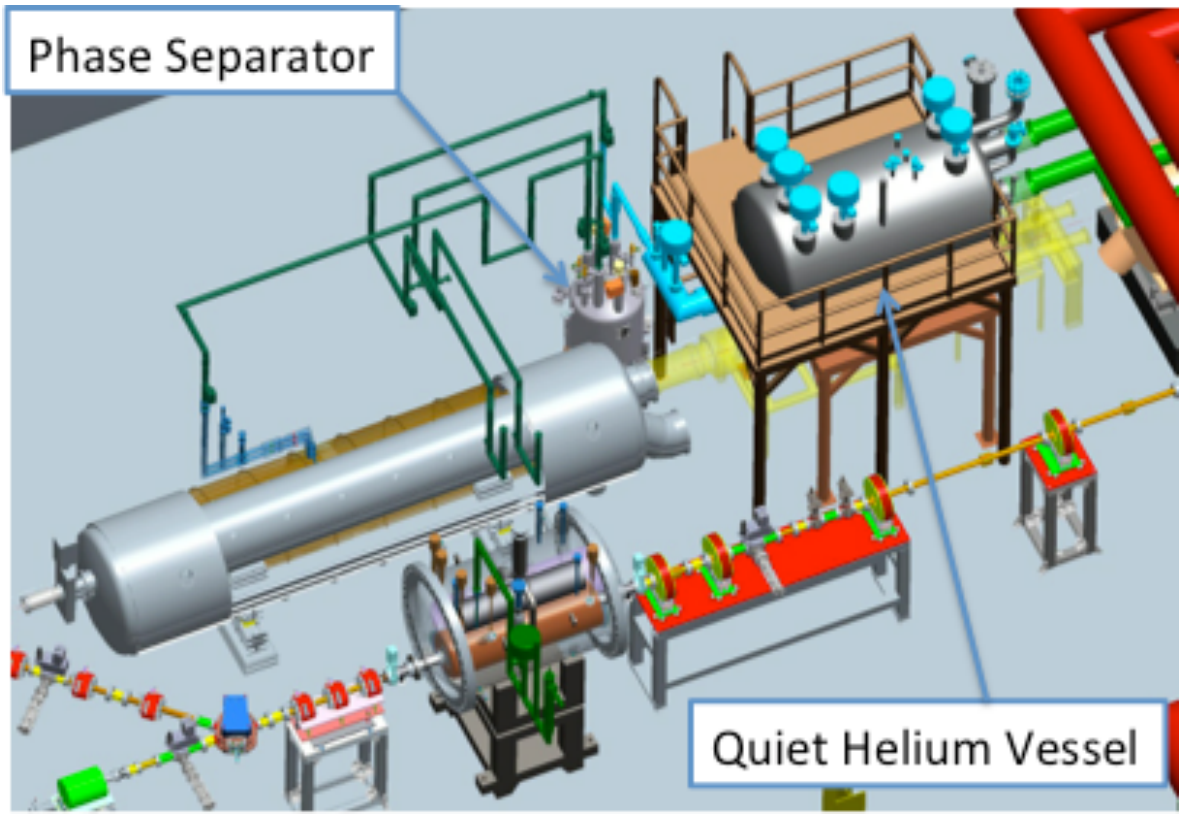

Fig. 16. Placement of phase separator and quiet helium vessel for 4K cryogenic system.

## VI. Electron Beam Transport

Three focusing solenoids – identical in the design to that used in R&D ERL - will be used to focus low energy electron beam in the beamline between the gun and the 20 MeV linac. The first solenoid will be mounted on the gun. The other two solenoids, placed between bunching cavities and accelerator, will be used as a pair fired in the opposite direction. Three power supplies for these solenoids are identical to that used in R&D ERL.

The rest of the optics provides for matching of the electron beam through the doglegs and into the FEL wiggler. As we mentioned in the introduction, quadrupoles located at the common trajectory of the ion and electron beams would focus electrons while being almost invisible for heavy ions.

The only common elements whose effect on the ion beam requires compensation are dipoles where the electron and ion beams are merged and separated. Two dipoles, identical to the merging and separating once, but with opposite direction of the magnetic field, are located on the ion-beam trajectory to null the effect on the ion beam. All focusing of the ion beam is provided by RHIC super-conducting quadrupoles located out-side of CeC section. The β-functions of the ion beam are identical in x- and y- directions, are symmetric with respect to the wiggler center where β-functions have minimum of $\beta^*$=5.5.

In contrast with steady behavior of ion beam size, the electron beam has to be matched into β=1m the helical wiggler as well as having a good overlap with ion beam in the kicker and the modulator sections.

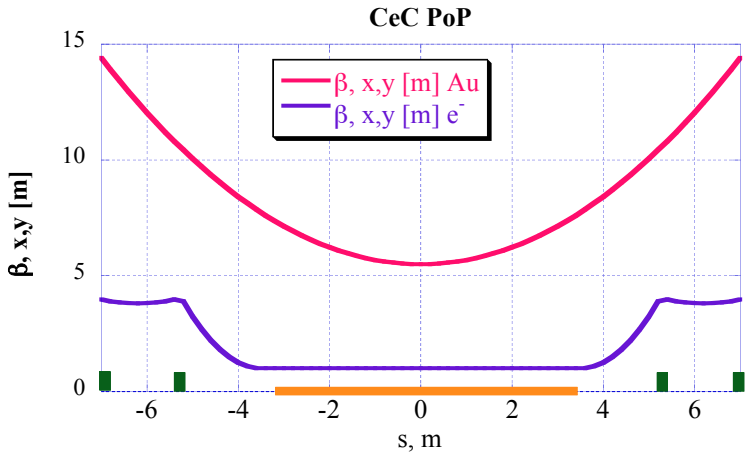


Fig. 17. Desirable β-functions for the ion and electron beams in the IP2 for our CeC experiment.

Preliminary optics functions of the e-beam are shown in figures 12 and 13. Fig. 12 shows beam optic of the beamline from the end of the 5-cell accelerator to the entrance of the wiggler. Three quadrupoles are used to match the e-beam into the first dogleg. Three dogleg quads provide for its achromaticity as well as a proper beam size at the entrance of the modulator section (β~6m). Four quads keep the beam-size of the e-beam through the modulator section and then focus it to required β=1m at the entrance of the helical wiggler.

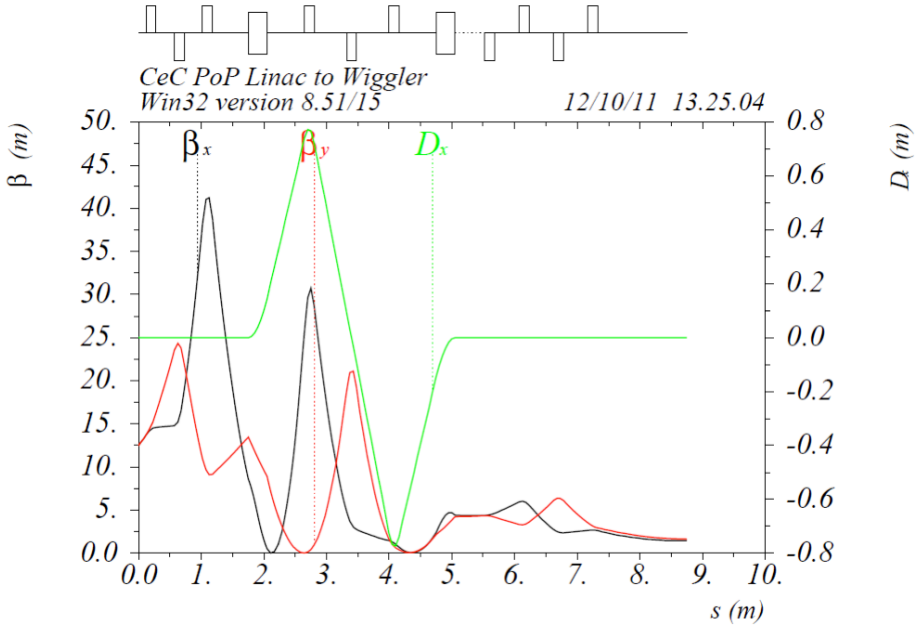


Fig. 18. 21.8 MeV e-beam optics from the exit of accelerator to the entrance to the wiggler.

After the wiggler, the e-beam matched by four quadrupoles into the kicker section. As seen in Fig. 13, the following dogleg with two quadrupoles serves as a beam spreader by blowing the e-beam size 10-fold. This expanding beam is absorbed in the dump.

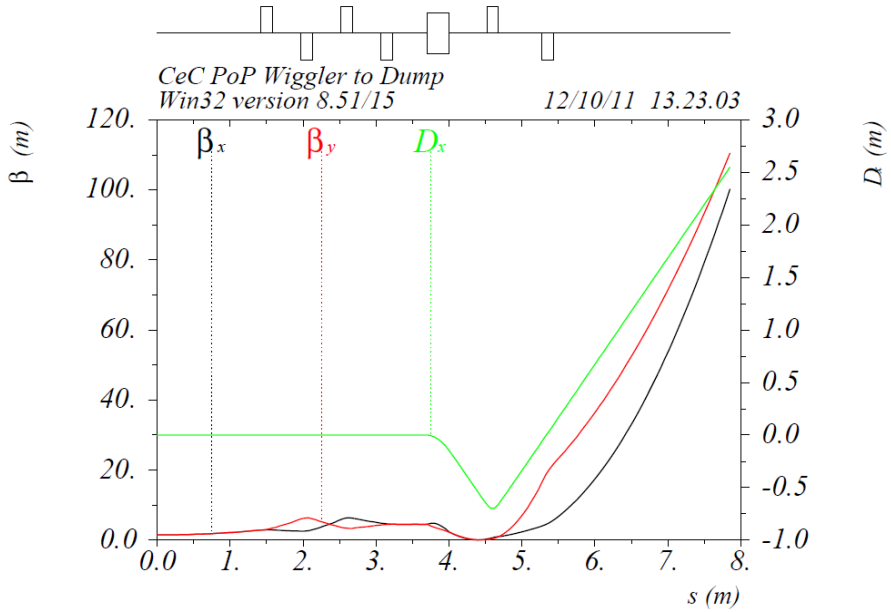


Fig. 19. 21.8 MeV e-beam optics from the exit of the wiggler to the beam dump.

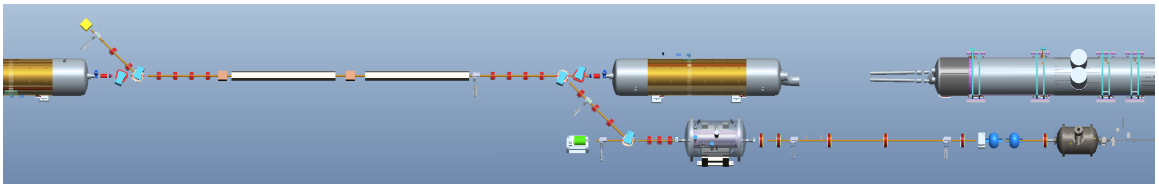

Fig. 20. Schematic of the CeC beam-line. Distances are approximate.

## VII. Magnets

### Dipole

Two dipoles form a dogleg to bring the e-beam to co-propagate with Yellow beam. The second dogleg takes the electron beam into the dump. Two additional dipoles, energized in opposite direction, compared with their neighbors, serve to make the CeC optics transparent of RHIC beams. All six dipoles will be fed in series by a single power supply. Each dipole will have individual 1% trim-coil. The dipole magnets, which design is shown in Fig. 21, will require water cooling.

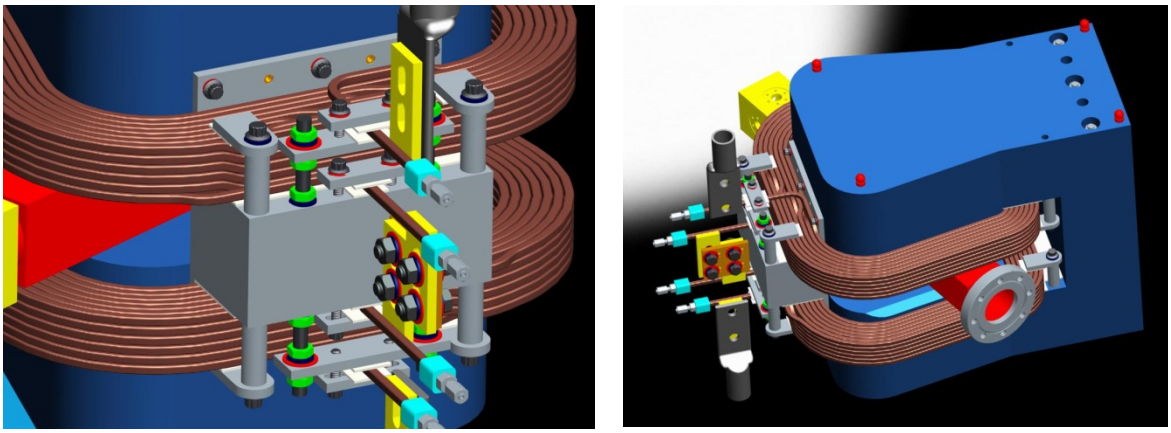

Fig. 21. View of the 45° dipole.

The dipole parameters are shown in Table 5.

Table 5. Parameters of the 45-degree dipole for CeC PoP experiment

| **Parameter** | **Value** |
|---|---|
| Core Length | 26.61 cm |
| Gap | 6 cm |
| Bend radius | 40.4 cm |
| Turn per pole | 42 |
| Good field region | ±2 cm |
| Magnetic length | 30.79 cm |
| Pole tip field | 1.902 kG |
| Maximal coil current | 140 A |
| Main coil resistance | 27.3 mOhm |
| | |
| | |

## Quadrupoles

We are using 16 quadrupoles to focus the 20 MeV electron beam. The design of the quadrupoles will be identical to that of R&D ERL, the quadrupole with ID of 2.362" (60 mm). The power supplies for the quadrupoles can be identical to that of that used in R&D ERL.

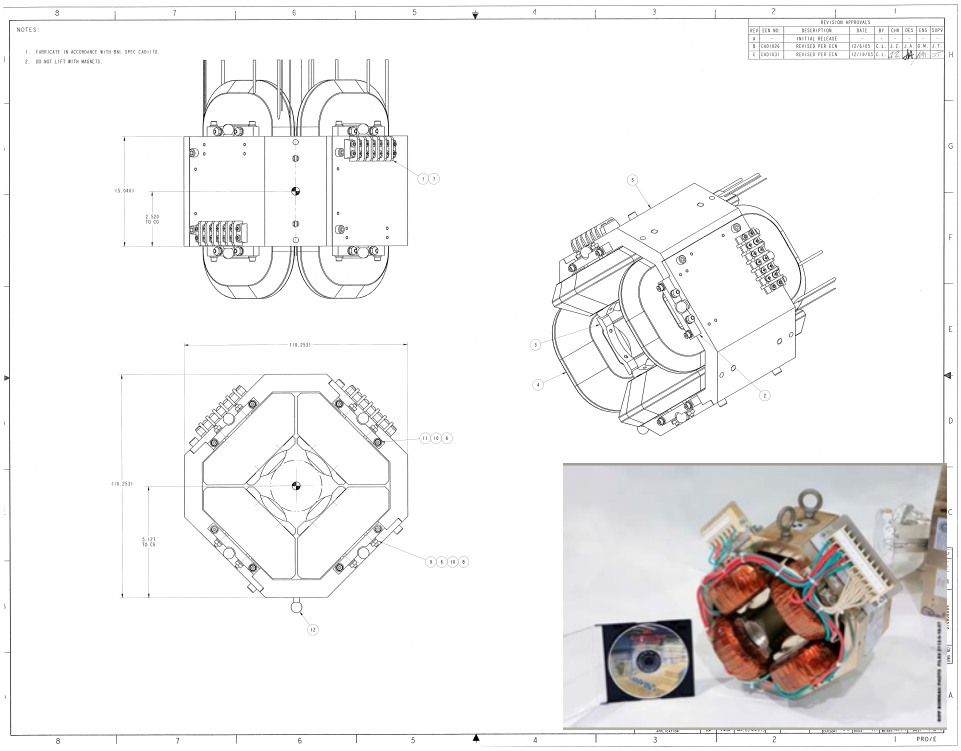

Fig. 22. General view of the quadrupole magnet.

Quadrupole will provide gradient up to 0.3 kGs/cm, and its magnetic length of about 16 cm. The field quality requirement is that 12-pole integral ratio is below $1.6\times10^{-4}$ at a radius of 2 cm.

The beam steering of the low energy electron beam will be performed with three dual plane corrector magnets. The maximal deflection angle is ±3 mrad (± 200 G cm). The 22 MeV electron beam will be steered using corrector coils in the quadrupoles.

## Solenoids

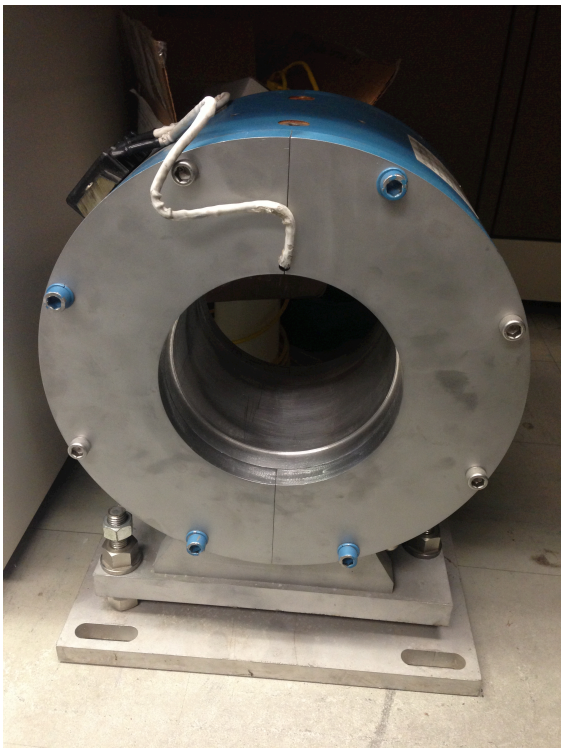

Fig. 23. View of the gun solenoid.

### Correctors

## VIII. Helical Undulator

BINP (Novosibirsk, Russia) has designed and manufactures a prototype of the helical undulator. The specifications for the undulator are shown in Table 6.

Table 6. Specifications for helical undulator

| Parameter | Value |
|---|---|
| Type | helical |
| Period | 4.0 cm |
| Gap | 32 mm |
| $a_W$ | 0.5 |
| Phase errors | < 1° r.m.s.,<br>< 3° peak |
| First integral | $< 30\times10^{-6}$ T m |
| Second integral | $< 30\times10^{-6}$ T m$^2$ |
| Length | 2.5 m |

Helical geometry provides equal focusing in both transverse directions and gives matched β=1m. The matched beam was used to simulate the amplification process in the

wiggler. The wiggler is designed with adjustable gap and can be reused for full size CeC cooler in RHIC/eRHIC operations.

At the end of the wiggler, we will install as simple electromagnetic compensated 3-pole wiggler to adjust the e-beam path length for about 25 microns. This wiggler should be designed and manufactured. Focusing of this weak device is negligible even for the electron beam.

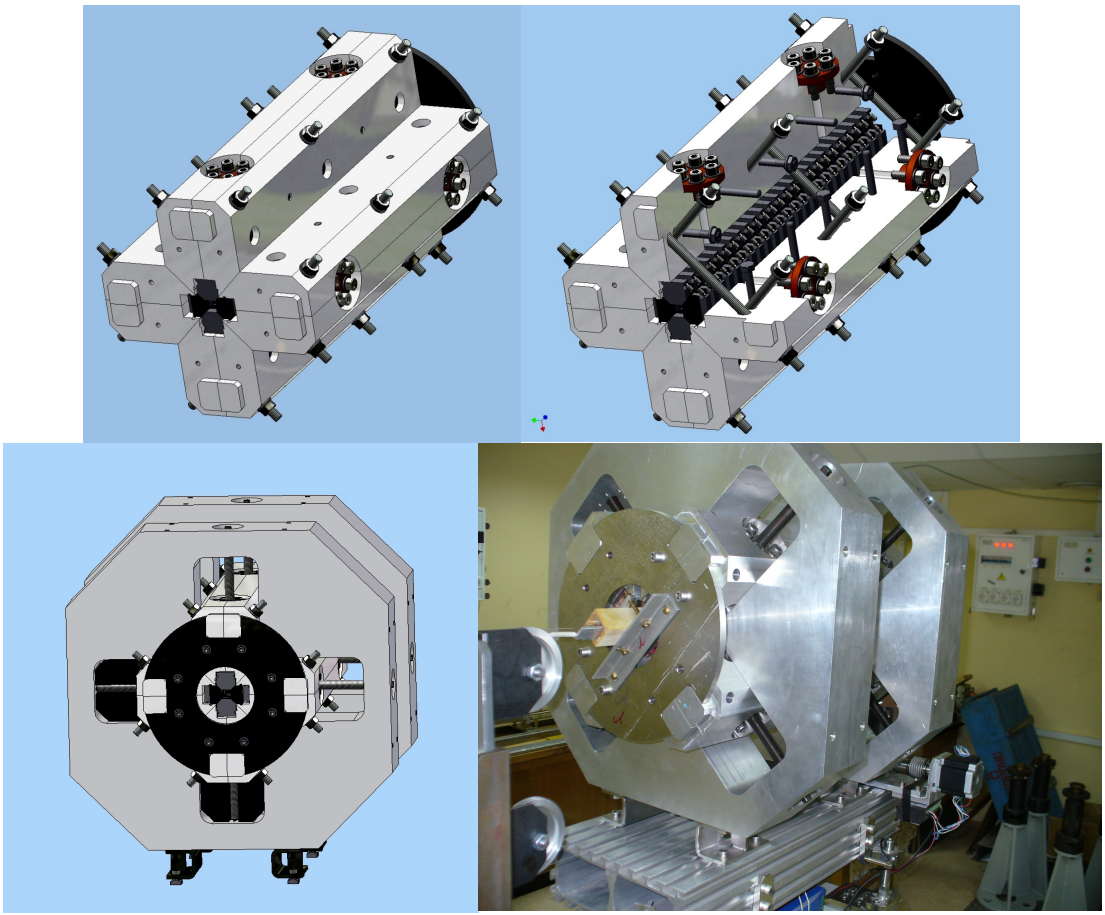

Fig. 24. Views of helical wiggler prototype.

## IX. Vacuum System

The vacuum system close to SRF cavities requires particulate-free vacuum system. The rest of the transport beam-line should have $10^{-9}$ Torr vacuum. The vacuum system of the CeC PoP beam-line should have two automatic valves at the ends of the doglegs to shut them off from RHIC vacuum in the case of unlikely vacuum accident.

The transport lines should have the pipe-size equal to that in the gun-to-linac (i.e. 2" ID). The only exception is a 4" pipe, which will connect the beam dump to the exit dogleg.

The helical wiggler opening has a square aperture with 32 mm opening. The wiggler will be installed with the 45-degree tilt to maximize the vertical aperture available for beam injection in RHIC.

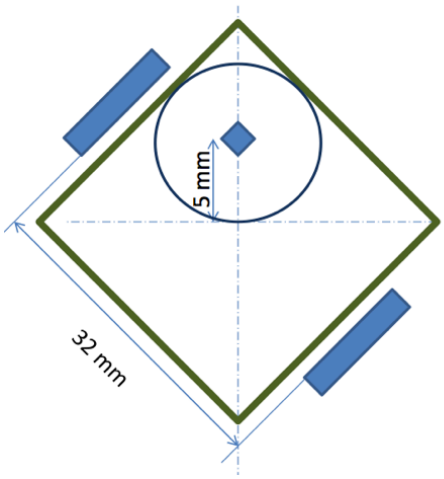


Fig. 25. Profile of the vacuum chamber in the helical wiggler. The vacuum chamber will be pressure-formed and the corners of the vacuum chamber will be rounded with about 4 mm radius.

## X. Beam Diagnostics

The electron beam diagnostics is very similar to that used for G5 test at R&D ERL. Preliminary list of the diagnostics is shown below:

1. Two in-flange Bergoz integrating current transformers (ICT) with beam charge monitors
2. Fluorescent screens (R&D ERL type) will be used for beam profile and position monitoring
3. Low energy emittance measurements system will utilize pepper-pot set-up
4. High energy emittance measurement system will utilize quadrupole scan
5. Beam Position Monitors
6. RHIC wall current monitor to monitor ion beam profile
7. Spectrum analyzer to monitor ion beam spectrum evolution
8. Infrared Radiation Diagnostics for FEL tuning utilizes 13 microns radiation from wiggler and include intensity detector and/or monochromator
9. Beam loss monitors to observe ion losses in the wiggler

### Integrating Current Transformer

We plan to utilize two in-flange integrating current transformers type CT-CF6-60.4-070-05:1-H-UHV. The transformer takes only 40 mm of space in the beamline and is shown in Fig. X.

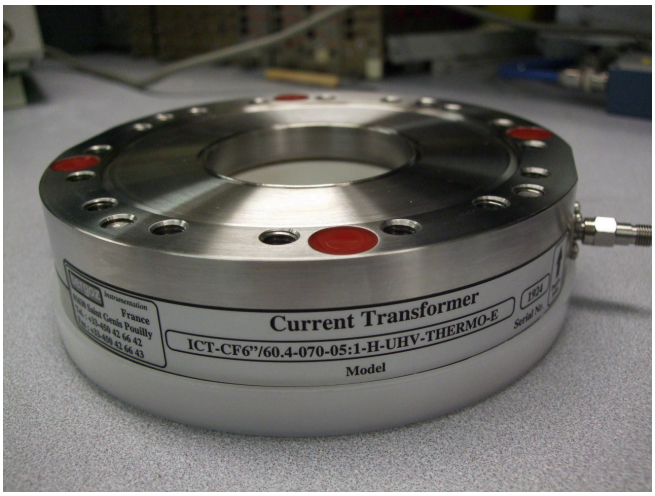

Fig. 26. View of the integrating current transformer.

The current (bunch charge) readout will be performed with Bergoz beam charge monitor integrate-hold-reset (IHR) type. This electronic is capable measuring of 10 kHz repletion rate, which is sufficient for the early stages and commissioning. During regular operations we will monitor only each eights bunch by providing the corresponding trigger rate.

## Fluorescent screens

The ion beam position will be monitored with existing RHIC pick-up electrodes (strip-lines). The electron beam position will be monitored with button type BPMs.

The flag resolution is 50 microns, which is sufficient to measure emittance of the beam. The flag will be placed on the extension of the beam-line after the first dipole. In such configuration the dispersion zero and does not affect emittance measurement. The flag in the dogleg will be used for energy spread measurement, and when acceleration off crest for the bunch length measurement. This flag will allow the measurement of sliced emittance. For this purpose the solenoids will be fed with opposite currents keeping the focusing the same but rotating beam in the XY plane.

The coarse synchronization between ion and electron bunches will be performed by observation signals form the RHIC and electron pick-ups on the oscilloscope.

The matching of the beam velocities (and the fine tuning of the synchronization) will be done by observation of the spontaneous radiation from the wiggler. The ions with significantly larger charge will produce larger shot noise coming from the electron beam due to the Debye screening.

The cooling effect will be observed by modification of the longitudinal profile of ion bunch. We expect to see a growth of the short peak with sub-nsec duration on the top of the 5-nsec profile of the ion bunch. The early detection of the cooling (or heating) of the central part can be detected by observing ion-bunch spectrum in the 1-3 GHz range. The ion beam-induced signal should come from the wall current monitor with nominal bandwidth from DC to 6 GHz.

We are considering a possibility of the port for launching of alignment laser beam for IR diagnostics.

## XI. Power Supplies

The five main dipole magnets are connected in series and one common power supply. All other magnets/winding are powered individually. Quadrupole trim wings are configured either as horizontal (in focusing quadrupoles) or vertical (in defocusing) correctors. All power supplies are controlled via Ethernet.

Table 7. Power supplies requirements

| **Function** | **Qty** | **I, Amps** | **V, Volts** | **Stability** |
|---|---|---|---|---|
| Main dipole | 1 | 167 | 30 | ±100 ppm |
| Quadrupoles | 16 | 10 | 20 | ±50 ppm |
| Gun solenoid | 1 | 15 | 40 | ±50 ppm |
| ERL solenoid | 5 | 10 | 40 | ±100 ppm |
| Correctors | 6 | ±5 | ±10 | ±100 ppm |
| Dipole & Quad trims | 19 | ±5 | ±20 | ±100 ppm |
| 3PW | 2 (3) | TBD | TBD | ±100 ppm |
| Undulator trims | 4 (6) | TBD | TBD | ±100 ppm |
| | | | | |

Two type of power supplies are expected to be employed. For low power CAENels model SY3634 will be used which are four bipolar regulators in a 3U crate with control module. The high power unit for the dipole is CAENels DiRAC model PS170030 which is a 6 kW unipolar converter. The unit is air-cooled and housed in a 3U rack.

Table 8. Power supplies specification

| | SY3634 | PS170030 |
|---|---|---|
| Set-point | 15 bits | 18 bits |
| Readback | 20 bits | 20 bits |
| Current ripple | 30 ppm FS | 100 ppm FS |
| Current stability | 50 ppm FS | 20 ppm FS |
| Accuracy | 0.05% | 0.1% |

## XII. Drive Laser

Choice of the multialkaline cathode defines the required laser parameters such as power and wavelength. Additional requirement, imposed on the laser system, is ability to vary length of the flat top part in the range 100-500 ps. We have chosen design of NuPhoton with a pulsed diode laser followed by an electro-optic modulator and Yb-doped fiber amplifier. The produced 1064 nm laser wavelength will be converted into the green light with second harmonic generator. The parameters of the lase are shown in Table 9.

Table 9. Parameters of the CeC PoP Drive Laser.

| Parameter | Value |
|---|---|
| Center wavelength | 532 nm |
| Center wavelength stability (24 hour) | 0.1 nm |
| Bandwidth | 0.1 nm |
| Repetition rate | 78.2±0.5 kHz |
| Peak power | > 1 kW |

| | |
|---|---|
| Pulse width (FWHM) | 100 – 500 psec |
| Pulse rise time | <100 psec |
| Pulse fall time | < 150 psec |
| Plateau flatness | ±9% |
| Jitter relative to trigger clock | < 10 psec |
| Pulse amplitude stability (5 minutes) | < 2% |
| Amplitude drift | < 5% |
| | |
| | |
| | |
| | |
| | |
| | |
| | |
| | |
| | |

## XIII. Control System

The control system will be located inside 3 racks containing 6 VME chassis: 2 for instrumentation, 2 for timing and power supply controls, 1 for laser an motion control, and 1 for RF systems motion control. Connection to the most devices (power supplies, cameras, vacuum and cryo controllers) will be done through the Ethernet. Machine protection will utilize 2 National Instruments RIO chassis and modules.

## References


[1] V. N. Litvinenko, Ya. S. Derbenev, Coherent Electron Cooling, Physical Review Letters 102, 114801 (2009), http://link.aps.org/abstract/PRL/v102/e114801.

[2] Vladimir N. Litvinenko, Johan Bengtsson, Ilan Ben-Zvi, Alexei V. Fedotov, Yue Hao, Dmitry Kayran, George Mahler, Wuzheng Meng, Thomas Roser, Brian Sheehy, Roberto Than, Joseph Tuozzolo, Gang Wang, Stephen Davis Webb, Vitaly Yakimenko, Andrew Hutton, Geoffrey Arthur Krafft, Matt Poelker, Robert Rimmer, George I. Bell, David Leslie Bruhwiler, Brian T. Schwartz, Proof-of-Principle Experiment for FEL-based Coherent Electron Cooling, Proceedings of 2011 Particle Accelerator Conference, New York, NY, USA, March 25-April 1, 2011, pp. 2064-2066, http://accelconf.web.cern.ch/AccelConf/PAC2011/papers/thobn3.pdf http://www.c-ad.bnl.gov/pac2011/proceedings/papers/thobn3.pdf

[3] C.226 Vladimir N. Litvinenko, Sergei Belomestnykh, Ilan Ben-Zvi, Jean C. Brutus, Alexei Fedotov, Yue Hao, Dmitry Kayran, George Mahler, Aljosa Marusic, Wuzheng Meng, Gary McIntyre, Michiko Minty, Vadim Ptitsyn, Igor Pinayev, Triveni Rao, Thomas Roser, Brian Sheehy, Steven Tepikian, Yatming Than, Dejan Trbojevic, Joseph Tuozzolo, Gang Wang, Vitaly Yakimenko (BNL, Upton, Long Island, New York),

Mathew Poelker, Andrew Hutton, Geoffrey Kraft, Robert Rimmer (JLAB, Newport News, Virginia), David L. Bruhwiler, Dan T. Abell, Chet Nieter, Vahid Ranjbar, Brian T. Schwartz (Tech-X, Boulder, Colorado), Pavel Vobly, Mikhail Kholopov, Oleg Shevchenko (Budker Institute of Nuclear Physis, Novosibirsk, 6300090, Russia), Peter Mcintosh,Alan Wheelhouse, (STFC, Daresbury Lab, Daresbury, Warrington, Cheshire, UK,WA4 4AD), Coherent Electron Cooling Demonstration Experiment, Proc. of Second International Particle Accelerator Conference, San Sebastian, Spain, September 4-9, 2011, p. 3442, http://accelconf.web.cern.ch/AccelConf/IPAC2011/papers/thps009.pdf

## Appendix A: Details of the ion interaction with electrons in CeC

In detail, within the modulator each individual ion attracts the surrounding electrons and generates an imprint of density modulation, as shown in Fig. A1. In about a quarter of plasma period, each ion becomes surrounded by a cloud of electrons with a total charge equal in value to its own, but opposite in sign, i.e., it is shielded. In the co-moving frame, the longitudinal velocity spread is significantly smaller than that in the transverse direction. Consequently, the Debye radius in transverse direction greatly exceeds that in the longitudinal direction, and the electron cloud assumes a very flat pancake-like shape.

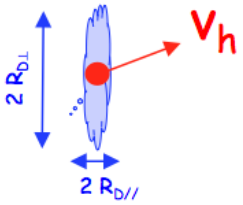


Fig. A1. In the modulator, each ion generates an individual imprint on the density of the electrons, taking the form of ellipsoid with the typical dimensions of the corresponding Debye radii.

These individual density modulations are self-amplified when electron beam passes through a high-gain FEL into a wave-packet in the electrons density (Fig. A2 ).

This periodic density-modulation generates a periodic longitudinal electric field. When the hadron recombines with the electron beam, it is exposed to this self-induced longitudinal electric field. We select the delay between the self-induced wave-packet and an ion in such a way that an ion with designed energy ($E_o$) arrives at the kicker on the top of the electron-density peak (Fig. A3), where electric field is zero. Hence, it does not experience any change in its energy.

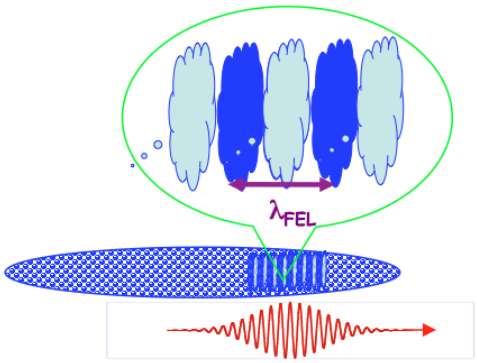


Fig. A2 In the FEL, the modulation of the e-beam's density is amplified into a wave-packet, i.e., into a series of "pancakes" with increased and reduced density of electrons.

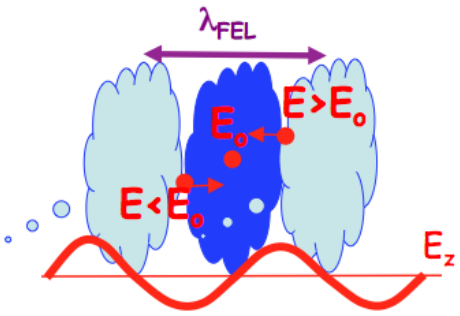


Fig. A3. In the kicker, the hadron interacts with its self-induced electric field. Depending on the sign of its energy deviation from the design value, Eo, hadron either is accelerated or decelerated.

Because ion's velocity depends on its energy, a time-of-flight for ion is also dependent on its energy. Thus, a hadron with higher energy than the designed value reaches the kicker ahead of the negatively charged (high density) peak, and is dragged back (decelerated) by its self-induced electric field. Similarly, a hadron with lower energy than designed energy enters the kicker behind the negatively charge (high density) peak and is pulled forward (accelerated) by the self-induced electric field. The outcome of this process is a reduction in the energy spread of the hadrons, and the consequent longitudinal cooling of the hadron beam.

This is as far one can go with hand-waiving and equation-less description of the CeC process.